Journal of Physiology (2002), **538.2**, *pp.* 619–631
DOI: 10.1013/jphysiol.2001.12888

www.jphysiol.org

Sleep–waking discharge patterns of neurons recorded in the rat perifornical lateral hypothalamic area

Md. Noor Alam *†, Hui Gong *†, Tarannum Alam *†, Rajesh Jaganath *, Dennis McGinty *† and Ronald Szymusiak *‡

** Research Service, V.A. Greater Los Angeles Healthcare System, North Hills, CA 91343, † Department of Psychology and ‡ Departments of Medicine and Neurobiology, School of Medicine, University of California, Los Angeles, CA 90024, USA*

The perifornical lateral hypothalamic area (PF-LHA) has been implicated in the control of several waking behaviours, including feeding, motor activity and arousal. Several cell types are located in the PF-LHA, including projection neurons that contain the hypocretin peptides (also known as orexins). Recent findings suggest that hypocretin neurons are involved in sleep–wake regulation. Loss of hypocretin neurons in the human disorder narcolepsy is associated with excessive somnolence, cataplexy and increased propensity for rapid eye movement (REM) sleep. However, the relationship of PF-LHA neuronal activity to different arousal states is unknown. We recorded neuronal activity in the PF-LHA of rats during natural sleep and waking. Neuronal discharge rates were calculated during active waking (waking accompanied by movement), quiet waking, non-REM sleep and REM sleep. Fifty-six of 106 neurons (53 %) were classified as wake/REM-related. These neurons exhibited peak discharge rates during waking and REM sleep and reduced discharge rates during non-REM sleep. Wake-related neurons (38 %) exhibited reduced discharge rates during both non-REM and REM sleep when compared to that during waking. Wake-related neurons exhibited significantly higher discharge rates during active waking than during quiet waking. The discharge of wake-related neurons was positively correlated with muscle activity across all sleep–waking states. Recording sites were located within the hypocretin-immunoreactive neuronal field of the PF-LHA. Although the neurotransmitter phenotype of recorded cells was not determined, the prevalence of neurons with wake-related discharge patterns is consistent with the hypothesis that the PF-LHA participates in the regulation of arousal, muscle activity and sleep–waking states.

(Received 25 June 2001; accepted after revision 28 September 2001)
Corresponding author R. Szymusiak: Research Service (151A3), V.A. Greater Los Angeles Healthcare System, 16111 Plummer Street, North Hills, CA 91343, USA. Email: rszym@ucla.edu

The perifornical lateral hypothalamic area (PF-LHA) has been implicated in several physiological functions, including feeding, energy homeostasis, locomotor activity, cardiovascular regulation and sleep–wake control. Lesions of the PF-LHA and surrounding areas produce a syndrome of aphagia and adipsia (Teitelbaum & Epstein, 1962), akinesa (Levitt & Teitelbaum, 1975), sensory deficits (Marshall & Teitelbaum, 1974) and enhanced synchronization of the neocortical EEG (de Ryck & Teitelbaum, 1978; Shoham & Teitelbaum, 1982). Injections of neuropeptide Y into the PF-LHA increase feeding (Stanley *et al.* 1985) and administration of catecholamines into this region can suppress food intake (Leibowitz, 1986). Electrical stimulation of the PF-LHA evokes locomotor activity (Sinnamon *et al.* 1999), EEG activation (Krolicki *et al.* 1985) and increased blood pressure and heart rate (Stock *et al.* 1981).

The PF-LHA contains neurons that have widespread projections throughout the brain and spinal cord. One type of projection neuron contains the peptide melanin concentrating hormone (MCH). These neurons are principally localized in the PF-LHA and zona incerta (Bittencourt *et al.* 1992, 1998). Other PF-LHA projection neurons contain the hypocretin (Hcrt) peptides (also known as orexins). Hcrt-producing neurons are localized in the PF-LHA and dorsomedial hypothalamic nucleus (de Lecea *et al.* 1998; Peyron *et al.* 1998; Sakurai *et al.* 1998; Nambu *et al.* 1999). Although MCH- and Hcrt-immunoreactive neurons are intermingled within the PF-LHA, these peptides are not co-localized within individual neurons (Broberger *et al.* 1998; Peyron *et al.* 1998). Intracerebroventricular adminstration of both MCH and Hcrt promotes food intake (Qu *et al.* 1996; Sakurai *et al.* 1998) and food restriction results in elevated levels of mRNA for both families of peptide (Qu *et al.* 1996; Yamamoto *et al.* 2000).

The Hcrt peptides have recently been implicated in the regulation of arousal and in the neuropathology of

narcolepsy. Narcolepsy is a neurological disorder characterized by excessive sleepiness and cataplexy (sudden loss of muscle tone precipitated by emotion; Siegel, 2000). A mutation of the Hcrt-2 receptor gene has been implicated in canine narcolepsy (Lin *et al.* 1999). Hcrt peptide knock-out mice exhibit cataplexy-like episodes, increased amounts of rapid eye movement (REM) and non-REM sleep and shorter waking episodes during the dark portion of the light–dark cycle (Chemelli *et al.* 1999). Hcrt mRNA is undetectable in the hypothalamus, pons and cortex of the brains of human narcoleptics (Peyron *et al.* 2000) and the number of Hcrt-immunoreactive neurons is reduced by 85–95 % in the hypothalamus of human narcoleptics (Thannickal *et al.* 2000).

Pharmacological studies support a role for Hcrt in the modulation of sleep–waking states. Intracerebroventricular infusion (Piper *et al.* 2000) or local microinjection of orexin into the target sites such as the preoptic area (Methippara *et al.* 2000) or locus coeruleus (Bourgin *et al.* 2000) promotes waking and suppresses REM sleep. Hcrt-1 application increases the discharge of rat locus coeruleus neurons *in vitro* (Hagan *et al.* 1999; Horvath *et al.* 1999). Immunoreactivity for c-fos protein is elevated in rat PF-LHA Hcrt and non-Hcrt neurons in response to systemic administration of the stimulant drug modafanil (Scammell *et al.* 2000), and in response to sustained wakefulness (Estabrooke *et al.* 2001).

The electrical activity of PF-LHA neurons during natural sleep and waking has not been described. The above findings led to the hypothesis that Hcrt-producing neurons are activated during wakefulness and deactivated during sleep. Here, we describe the frequency and distribution of sleep–wake-related discharge patterns of neurons recorded extracellularly within the field of Hcrt-immunoreactive neurons in the rat PF-LHA. Recorded neurons were grouped on the basis of the ratio of discharge rates during REM sleep and waking in anticipation of the possibility that a subset of PF-LHA neurons (specifically, those containing Hcrt) might exhibit differential activation during these two behavioural states.

METHODS

Experimental subjects and surgical procedures

We used seven male Sprague-Dawley rats weighing 300–350 g, maintained on a 12 h:12 h light–dark cycle (lights on at 08.00 h) with food and water freely available. Unit recordings of suitable quality were obtained from five of the rats. All experiments were conducted in accordance with the National Research Council Guide for the Care and Use of Laboratory Animals and all procedures were reviewed and approved by the Internal Animal Care and Use Committee of the V.A. Greater Los Angeles Healthcare System.

Rats were surgically prepared for chronic recording of extracellular neuronal activity in the PF-LHA and electrographic assessment of sleep–waking states as described by Alam *et al.* (1997). In brief, neocortical EEG and dorsal neck EMG electrodes were implanted aseptically under anaesthesia (ketamine + xylazine, 80:10 mg kg^{-1}, I.P.) for polygraphic determination of the sleep–waking state. A single barrel (23 gauge stainless steel tube) mechanical microdrive was implanted stereotaxically such that the tip rested 3 mm above the dorsal aspect of the PF-LHA (A, −2.9 to −3.3; L, 1.2; H, −4.8 to 5.0; Paxinos & Watson, 1998). Five pairs of microwires, each consisting of two 20 μm insulated stainless steel wires glued together except for 2.0 mm at the tip, were inserted into the barrel such that the tips projected into the PF-LHA.

Data acquisition

Experiments were carried out after allowing at least 7 days for recovery from surgery. During the recovery period, animals were placed for 2–3 h per day in an electrically shielded, sound attenuated recording chamber (temperature: 25 ± 2 °C) and acclimatized to the recording environment. On experimental days, recordings were performed during the light portion of the light–dark cycle between 09.00 h and 15.00 h. During the recording session, the microdrive was advanced by 25–30 μm steps until amplified microwire signals, as confirmed in oscilloscopic traces, showed the presence of action potentials with a signal to noise ratio $\geqslant$ 2.0. Microwire recordings were filtered between 10 Hz and 5 kHz. The sampling rate was 25 000 samples s^{-1}. EEG and EMG recordings were digitized at a sampling rate of 220 samples s^{-1} and stored for subsequent off-line analysis of sleep and waking state-dependent unit activity.

Individual action potentials were sorted from filtered, amplified microwire recordings on the basis of spike shape parameters using Spike 2 software (Cambridge Electronic Design 1401, London, UK). Spike 2 software was used to produce templates based on waveform amplitude and shape for each distinct action potential present in the raw signal and to sort action potentials throughout the recording by matching them with these templates. Spike shapes were based on 135 analog to digital sampling points. All spikes that did not match existing templates were stored for subsequent off-line examination to ensure that such spikes were not incorrectly rejected. To minimize the possibility that spikes from multiple cells matched a single template, interspike interval histograms were constructed for each discriminated unit to verify that no intervals < 2 ms were recorded.

The discharge rate of each discriminated PF-LHA neuron was recorded through three to five stable sleep–wake cycles (~60–180 min). After completion of these recordings, the microdrive was advanced again in an attempt to isolate additional units for study. This sequence was repeated 2–3 times during a 6 h period.

Histology

At the end of a recording session, animals were deeply anaesthetized (pentobarbital, 100 mg kg^{-1}, I.P.,), injected with heparin (500 U, I.P.) and perfused transcardially with 30–50 ml of 0.1 M phosphate buffer (pH 7.4) followed by 300 ml of 4 % paraformaldehyde and 100 ml of 10 and 30 % sucrose in phosphate buffer. The brains were removed and equilibrated in 30 % sucrose solution and then freeze-sectioned at 40 μm thickness. Immunohistochemistry for Hcrt-1 was performed on every third section in three rats. Sections were treated with 0.6 % H_2O_2, rinsed in Tris-buffered saline (TBS) and incubated in blocking solution (0.2 % Triton X-100 and 4 % normal goat serum in TBS) for 2 h at 4 °C. The sections were then rinsed in TBS and incubated in the primary antisera, namely rabbit polyclonal

anti-Hcrt-1 (Oncogene, USA) diluted 1:2000 in diluent (0.1 % Triton X-100 and 4 % normal goat serum in TBS) for 48 h at 4 °C. The sections were then rinsed in TBS and incubated in diluent containing goat anti-rabbit IgG (1:250, Vector Laboratories, USA) for 2 h and then rinsed and incubated in avidin–biotin peroxidase (1:100 in TBS, ABC Elite Kit, Vector Laboratories) for 2 h at room temperature. Sections were then rinsed in 0.05 M Tris buffer, treated for 5–10 min with 0.05 % diaminobenzidine (Vector Laboratories) and 0.001 % hydrogen peroxide in 0.05 M Tris buffer, and then rinsed in TBS. Staining was absent from control sections from each brain processed without primary antibody. The tracks of the microwire bundles were identified histologically and the locations of recorded neurons were reconstructed along each track (Fig. 1*A*). Individual microwires in a bundle could be separated by a maximum of 125 μm in laterality, depth or anterior–posterior plane. Because the location of individual microwires in a bundle could not be determined, the reconstructed locations of recorded neurons were subject to this potential error. The reconstructed locations of recorded neurons and Hcrt-1-immunoreactive neurons were plotted side by side on the same section to determine whether the locations of recorded neurons and Hcrt-1-immunoreactive neurons were congruent (Fig. 1*B* and *C*).

Data analysis

States of active waking (AW), quiet waking (QW), non-REM sleep and REM sleep were identified on the basis of EEG and EMG patterns using standard criteria (Timo-Iaria *et al.* 1970). Mean discharge rates of individual neurons during AW, QW, non-REM sleep and REM sleep were calculated from 40–300 s blocks of three to five stable recording episodes from each state. The discharge rate during REM sleep was calculated from all episodes that were longer than 20 s. Seven of 113 recorded neurons exhibited very

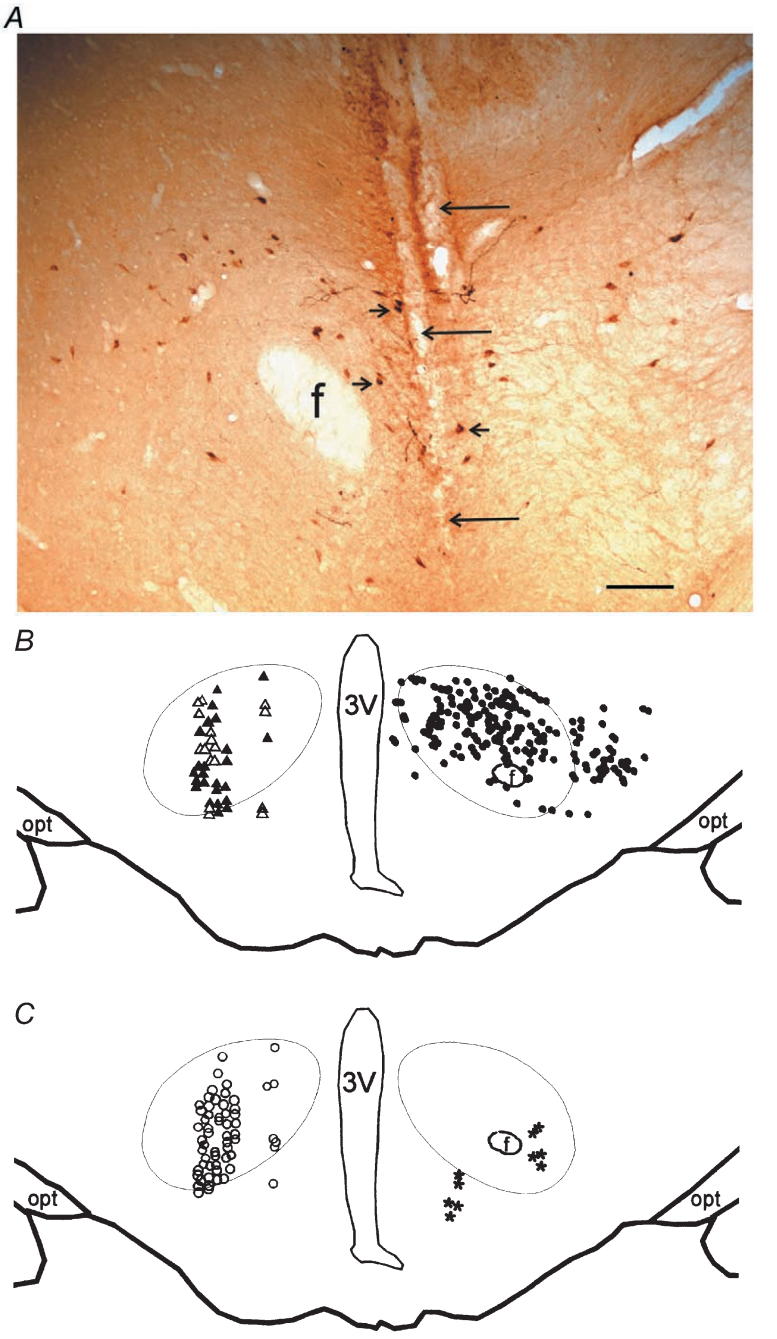

Figure 1. Distribution of Hcrt-immunoreactive neurons and locations of recorded neurons in the rat PF-LHA

A, photomicrograph of a representative coronal section through the PF-LHA showing the microwire tracts (long arrows) and Hcrt-1-immunoreactive neurons (short arrows). Scale bar, 100 μm. *B*, camera lucida drawing of a representative coronal section through the PF-LHA showing the distribution of Hcrt-immunoreactive neurons on the right side (●). The area delineated by the thin line indicates the highest density of Hcrt neurons in PF-LHA regions where neuronal recordings were performed. This area has been reproduced on the left side in *B* and *C* to indicate the location of recorded neurons with respect to Hcrt neurons. The locations of Type I wake-related (▲) and Type II wake-related (△) neurons are plotted on the left side in *B*. Note that nearly all of the recorded wake-related neurons were localized in or immediately adjacent to the Hcrt-immunoreactive neuronal field. *C*, camera lucida drawing of the same section depicted in *B*, showing the distribution of wake/REM-related neurons (○) on the left side and REM-related neurons (∗) on the right side. Abbreviations: 3V, third ventricle; f, fornix; opt, optic tract.

slow firing (< 0.5 Hz) in all sleep–waking states and were excluded from subsequent analyses.

Preliminary examinations of PF-LHA unit activity revealed several types of sleep–wake discharge patterns among recorded neurons. Therefore, it was necessary to segregate neurons according to their sleep–wake discharge profile to permit meaningful statistical comparisons among groups of neurons. We decided to segregate neurons based on the value of the ratio of discharge rates during REM sleep *vs.* waking (REM/wake ratio). This parameter was selected because there is physiological evidence that Hcrt-producing neurons in the PF-LHA are activated during waking, but might exhibit suppression of discharge during REM sleep. Classification of neurons on the basis of the REM/wake ratio allowed us to distinguish neurons with this discharge pattern from those that are activated during both waking and REM sleep, a cell type commonly encountered in the lateral hypothalamus of cats and rats (Szymusiak *et al.* 1989; Krilowicz *et al.* 1994; Steininger *et al.* 1999).

Neurons were classified as wake related if the REM/wake ratio was < 0.5. Two types of wake-related neurons were defined, based on the magnitude of the suppression of discharge during REM sleep. Type I wake-related neurons displayed a REM/wake ratio ⩽ 0.2. Type II wake-related neurons displayed a REM/wake ratio > 0.2 and < 0.5. Neurons were classified as wake/REM-related if the REM/wake ratio was ⩾ 0.5 and < 1.5. Neurons were classified as REM related if the REM/wake ratio was ⩾ 1.5. The effects of sleep–waking state on the discharge rate of each class of neuron were assessed with a one-way repeated measures ANOVA. The significance of differences between individual sleep-wake state means was evaluated with Newman-Keuls *post hoc* tests.

The duration of each discriminated action potential was calculated from averaged waveforms (based on 10–30 action

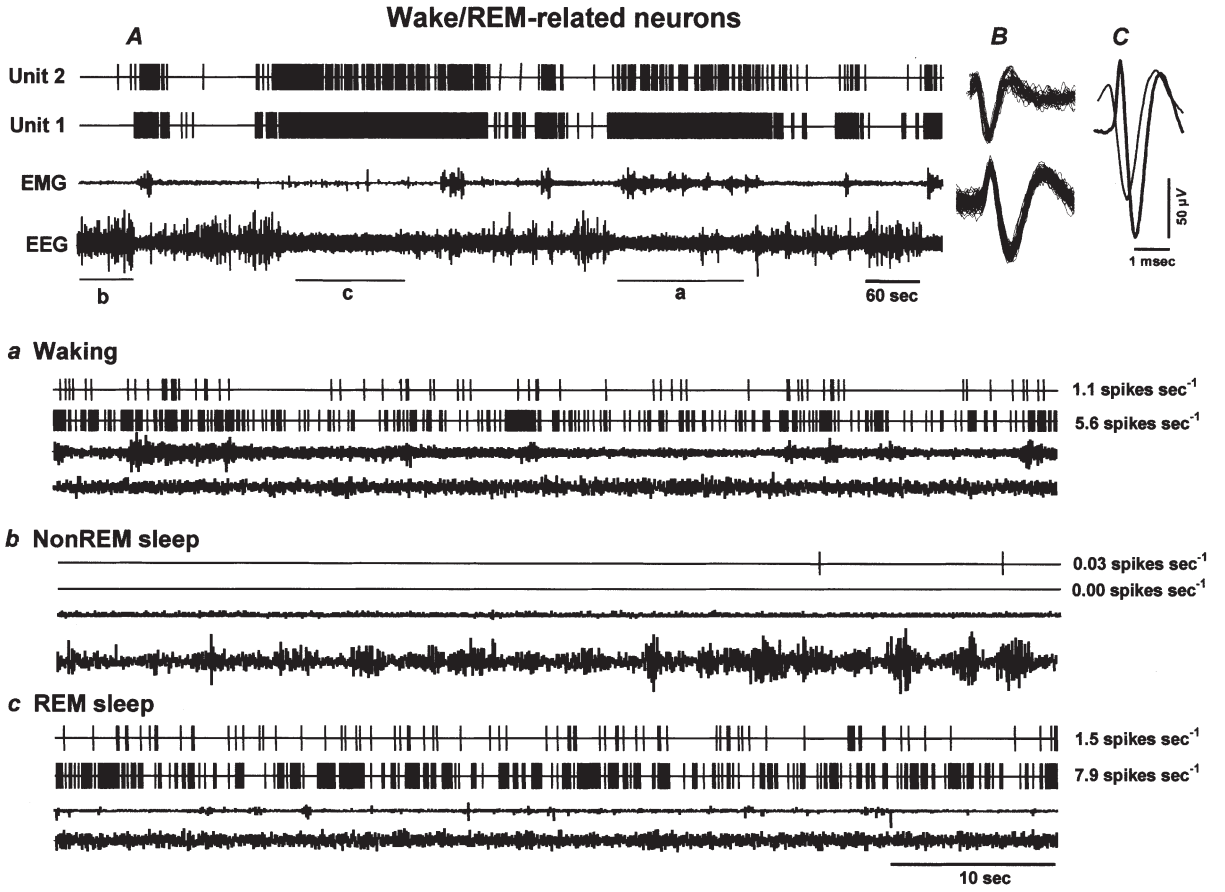

Figure 2. The discharge pattern of individual wake/REM-related neurons across the sleep–waking cycle

A, 15 min of continuous recording showing the discharge of two wake/REM-related neurons (Units 1 and 2) recorded simultaneously across the sleep–waking cycle. *B*, the superimposed waveforms of individual action potentials of the recorded neurons captured during five consecutive seconds along with the background signal variations. *C*, the averaged waveforms of the two action potentials recorded for five consecutive seconds. Note the difference in the spike shape and the duration of the action potentials, even though these neurons were recorded simultaneously from the same microwire. Lower panels illustrate expanded tracings (60 s) from *A*, showing the discharge patterns of the recorded neurons during waking (*a*), non-REM sleep (*b*) and REM sleep (*c*). The values to the right of each expanded tracing represent mean discharge rates (spikes s^{-1}) for the respective neurons during the representative sections. These neurons exhibited high discharge rates during waking and REM sleep and dramatically reduced discharge rates during non-REM sleep. EEG, electroencephalogram; EMG, neck electromyogram.

potentials) to reduce noise. The duration of an action potential was measured from the initial inflection from baseline voltage to the point at which the after-potential returned to the baseline (see Figs 2*C*, 4*C* and 6*C*). The effects of cell classification on action potential duration were assessed with a one-way ANOVA followed by a Newman-Keuls *post hoc* test.

The relationship of neuronal discharge to muscle activity was examined for each class of neuron. For 60–120 min recording periods containing episodes of waking, non-REM and REM sleep, discharge rates were calculated for successive 5 s epochs. These values were paired with the amplified, rectified dorsal neck EMG during the same epoch. Thus, multiple pairs of discharge rate *vs.* EMG activity values were generated across all sleep–waking states. Simple linear regression was calculated for each of the classified neuronal types. To plot these data, values were grouped on the basis of EMG activity into 0.3 V bins (see Fig. 8).

RESULTS

Anatomical location of recorded neurons

A total of 106 neurons recorded from dorsal to ventral passes through the PF-LHA were characterized by sleep and waking state-dependent discharge patterns. On the basis of the REM/wake discharge rate ratio, 56 neurons (53 %) were classified as wake/REM related, 24 (23 %) as Type I wake related, 16 (15 %) as Type II wake related and 10 (9 %) as REM related. A photomicrograph of a representative microwire pass in a Hcrt-immunostained PF-LHA section is shown in Fig. 1*A*. Figures 1*B* and *C* show the distribution of Hcrt-immunoreactive neurons in the vicinity of the microwire tracts and the location of each classified neuron. Hcrt-immunoreactive neurons were located in the perfornical lateral hypothalamus and dorsal medial hypothalamic area. The rostral–caudal plane of the recorded neurons varied by 0.1–0.4 mm through the PF-LHA but they have been superimposed on a single plane of the section illustrated in Fig. 1*B* and *C*. The different neuronal types encountered were not clearly segregated within the PF-LHA. Nearly all of the recorded neurons were located in the field of Hcrt-immunoreactive neurons.

The details of the discharge patterns and other characteristics of the different neuronal types encountered were as follows.

Sleep–waking state-related discharge patterns

Wake/REM-related neurons. This was the most frequently encountered class of neuron. Computer-generated tracings of the individual discharge patterns of two wake/REM-related neurons recorded simultaneously are shown in Fig. 2. The individual discharge rate (spikes s^{-1}) of all the recorded neurons during AW, QW, non-REM sleep and REM sleep and their mean discharge rate as a group are shown in Fig. 3*A* and *B*, respectively. These neurons had a mean (± S.E.M.) REM/wake ratio of 0.87 ± 0.04 (range, 0.51–1.48). There was a significant overall effect of sleep–waking state on the discharge rate of wake/REM-related neurons ($F_{3,55} = 31.2$, $P < 0.0001$). The discharge rate in AW was significantly higher than in QW and non-REM sleep, but did not differ significantly from that in REM sleep (Fig. 3*B*). REM sleep rate was also significantly higher than rates during QW and non-REM sleep. The discharge rate during QW was significantly higher than non-REM sleep rate.

Type I wake-related neurons. Computer-generated tracings showing the individual discharge patterns of two simultaneously recorded Type I wake-related neurons are shown in Fig. 4. The discharge rate of individual Type I

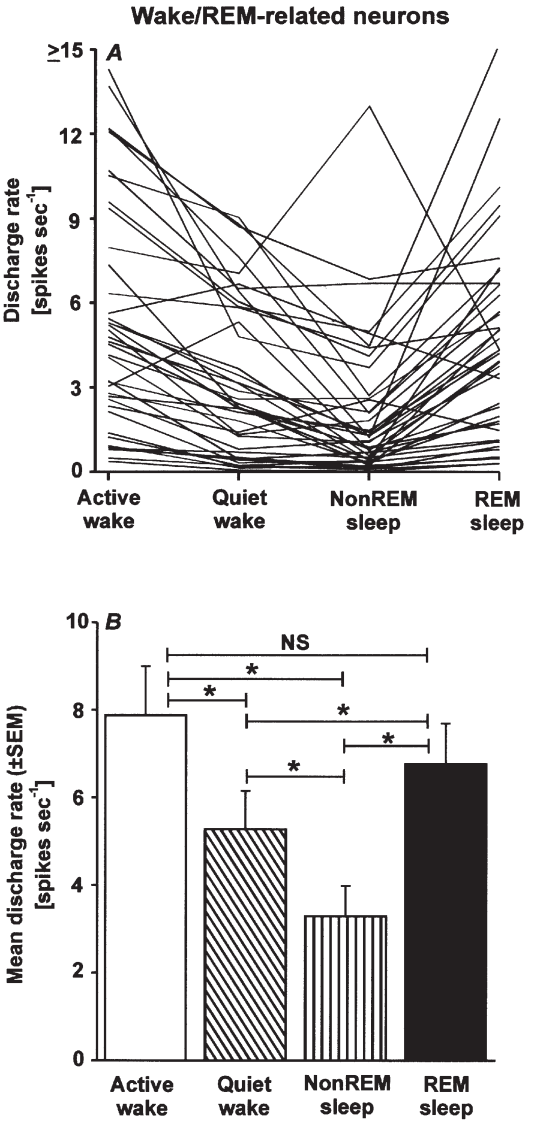

Figure 3. Discharge characteristics of wake/REM-related neurons

Individual (*A*) and mean (± S.E.M.; *B*) discharge rates (spikes s^{-1}) of wake/REM-related neurons during active waking (AW), quiet waking (QW), non-REM sleep and REM sleep. As a group, these neurons exhibited a significantly higher discharge rate during both AW and REM sleep when compared to QW and non-REM sleep. * $P < 0.01$. NS, not significantly different.

wake-related neurons and their mean discharge rate as a group are shown in Fig. 5*A* and *B*, respectively. Type I wake-related neurons exhibited a mean REM/wake ratio of 0.09 ± 0.01 (range, 0.003–0.200). There was a significant overall effect of sleep–waking state on discharge rates ($F_{3,23} = 38.5$, $P < 0.0001$). The discharge rate during AW was significantly higher than those in all other states. There were no significant differences in mean discharge rates during QW, non-REM sleep and REM sleep.

Wake-related discharge patterns that exhibit near cessation of activity during REM sleep are characteristic of several monoaminergic cell groups (see Introduction). A comparison of Type I wake-related neurons recorded in PF-LHA with putative serotonergic 'REM-off' neurons recorded in dorsal raphe of rats (Guzman-Marin *et al.* 2000) is presented in Table 1. These two classes of neuron exhibited similar declines in discharge rate during REM sleep compared to AW (91.09 ± 1.56 *vs.* 92.58 ± 8.35 %). However, PF-LHA wake-related neurons exhibited a significantly higher discharge rate during AW and a significantly greater reduction in discharge rate from AW to QW compared to dorsal raphe neurons. Dorsal raphe neurons exhibited a significant reduction in discharge rate from non-REM to REM sleep, whereas PF-LHA neurons did not. In addition, action potential durations of dorsal raphe neurons were significantly longer.

Type II wake-related neurons. The discharge rate of individual Type II wake-related neurons and their mean

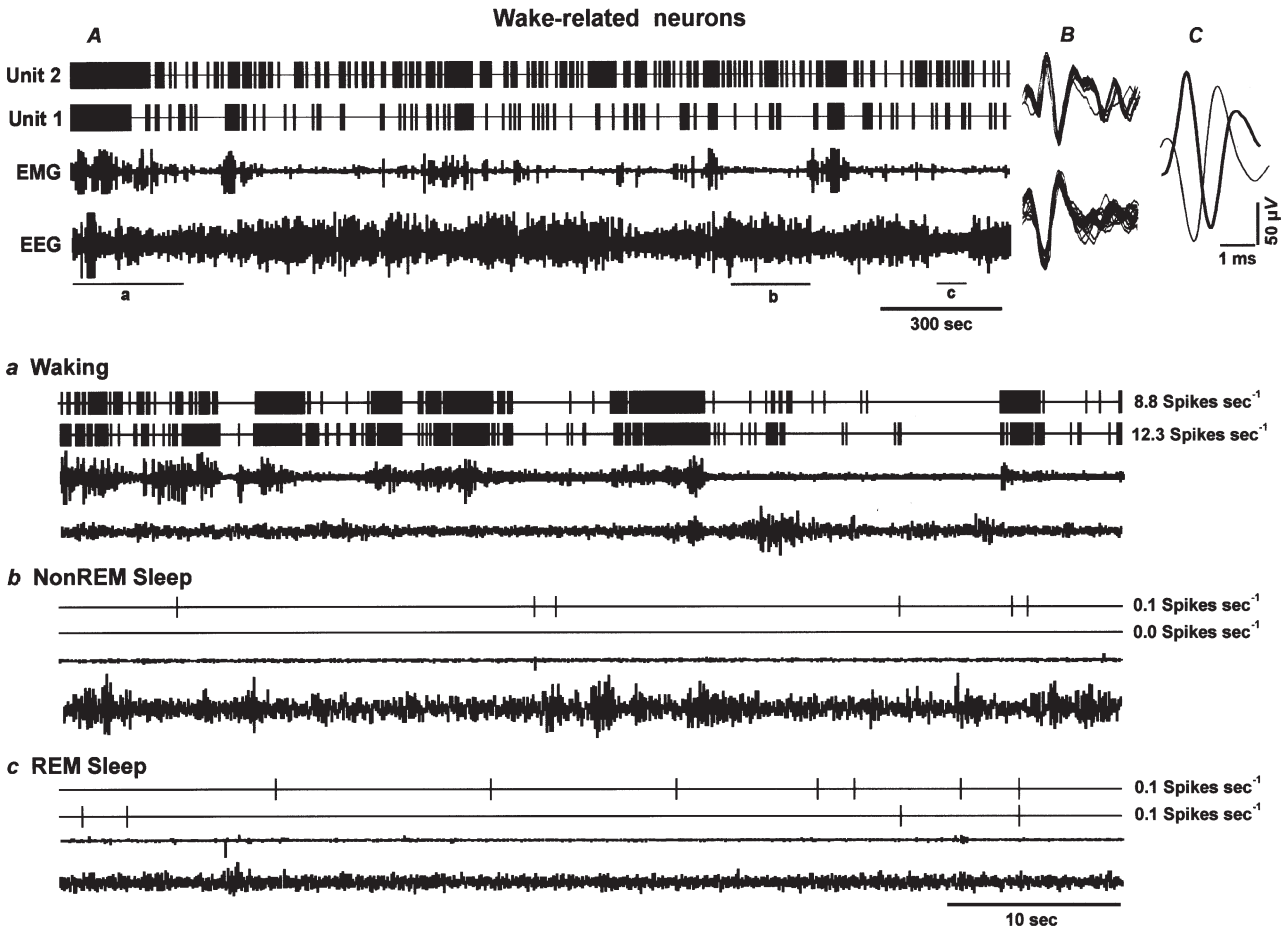

Figure 4. Discharge patterns of wake-related neurons across the sleep–waking cycle

A, 66 min tracing showing continuous discharge of two Type I wake-related neurons (Units 1 and 2) recorded simultaneously across the sleep–waking cycle. The superimposed waveforms of individual action potentials captured during 5 s along with the background noise and their averaged waveforms are shown in *B* and *C*, respectively. Lower panels depict expanded tracings (60 s) showing discharge rates of these two neurons during waking (*a*), non-REM sleep (*b*), and REM sleep (*c*). Wake-related neurons exhibited highest discharge rates during AW, as indicated by desynchronized EEG and increased EMG activity, a dramatic decline in discharge rates during QW and a further decline during non-REM sleep and REM sleep. The values to the right of each expanded tracing represent the mean discharge rate during the representative sections of the tracing.

Table 1. Comparison of sleep–wake discharge of Type I wake-related neurons recorded in the PF-LHA and wake-related/'REM-off' neurons recorded in rat dorsal raphe nucleus

Area	AW (spikes s^{-1})	QW (spikes s^{-1})	Non-REM sleep (spikes s^{-1})	REM sleep (spikes s^{-1})	Decrease from wake to REM sleep (%)	Decrease from AW to QW (%)	Spike width (ms)
Dorsal raphe ($n = 24$)	1.09 ± 0.14	0.69 ± 0.12	0.34 ± 0.04	0.09 ± 0.02	92.6 ± 8.0	38.4 ± 4.7	2.88 ± 0.09
PF-LHA ($n = 24$)	4.54 ± 0.70 *	1.03 ± 0.31	0.29 ± 0.09	0.37 ± 0.10	91.1 ± 1.5	77.5 ± 4.2 *	2.23 ± 0.07 *

Data for dorsal raphe neurons are taken from Guzman-Marin *et al.* (2000). All values are means ± S.E.M.
* $P < 0.01$ (independent two-tailed t test).

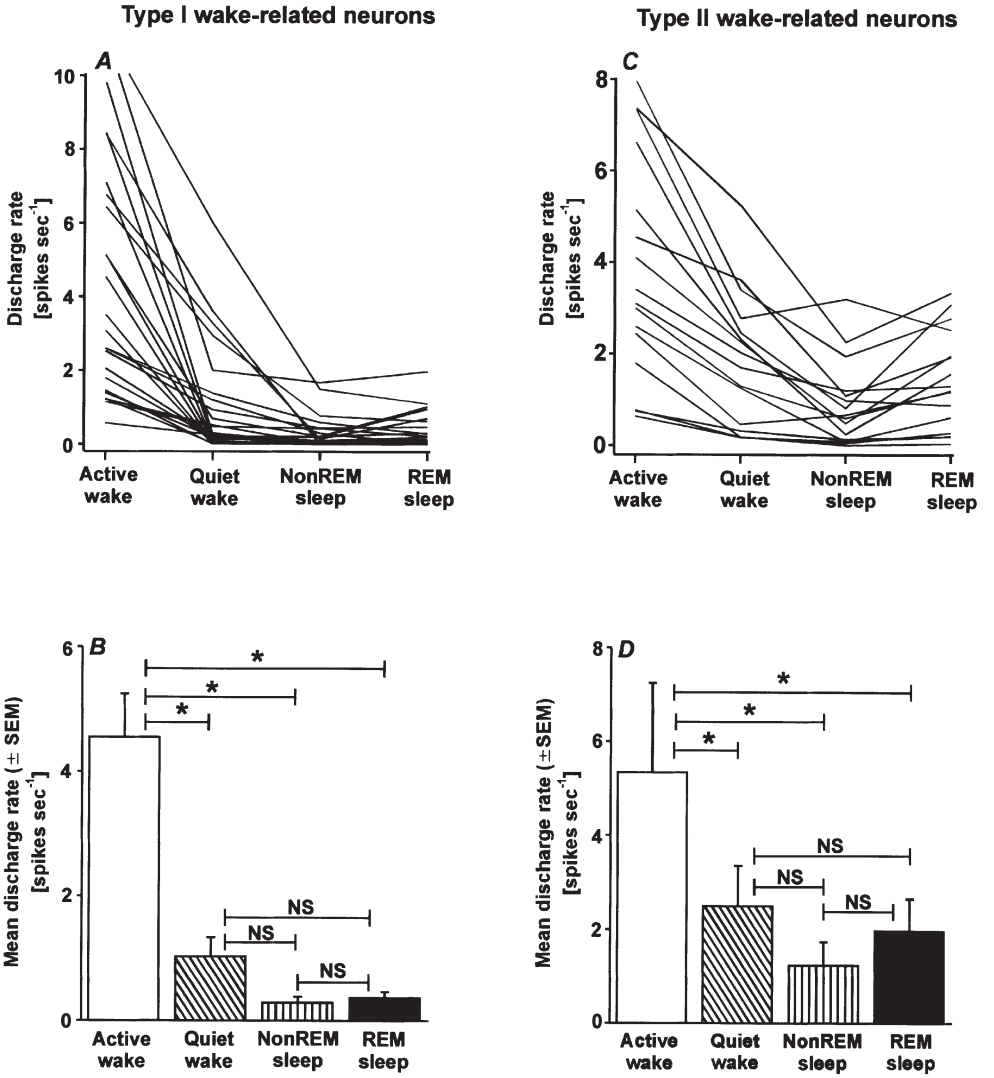

Figure 5. Discharge characteristics of Type I and II wake-related neurons

Activity of Type I (*A* and *B*) and II (*C* and *D*) wake-related neurons during AW, QW, non-REM sleep and REM sleep, showing individual (*A* and *C*) and mean (± S.E.M.; *B* and *D*) discharge rates. Note that both types of neuron exhibited significantly higher discharge rates during AW compared to QW, non-REM and REM sleep. For both types of neuron, discharge rates during QW, non-REM and REM sleep were not significantly different. * $P < 0.01$.

discharge rate as a group during AW, QW, non-REM sleep and REM sleep are shown in Fig. 5*C* and *D*, respectively. The mean REM/wake ratio was 0.35 ± 0.03 (range, 0.02–0.48). There was a significant overall effect of sleep–waking state on discharge rates ($F_{3,15} = 8.1$, $P < 0.001$). As in the case of Type I neurons, the discharge rate during AW was significantly higher than those in all other states and there were no significant differences in mean discharge rates during QW, non-REM sleep and REM sleep (Fig. 5*D*).

REM-related neurons. These neurons were the least frequently encountered type (10/106). Computer-generated tracings of individual discharge patterns from two REM-related neurons that were recorded simultaneously are shown in Fig. 6. The mean REM/wake ratio of REM-related neurons was 3.88 ± 1.10 (range, 1.99–12.97). Figure 7*A* and *B* shows the individual REM-related neuron discharge rates and their mean discharge rates during AW, QW, non-REM sleep and REM sleep. There was a significant effect of sleep–waking state on the discharge rates of these neurons ($F_{3,9} = 8.3$, $P < 0.001$). The discharge rate during REM sleep was significantly higher than those in all other states. There were no significant differences in mean discharge rates during AW, QW and non-REM sleep (Fig. 7*B*).

Action potential duration

Mean action potential duration was 1.84 ± 0.4 ms (range, 1.04–2.24 ms) for wake/REM-related neurons, 2.23 ± 0.08 ms (range, 1.6–3.12 ms) for Type I wake-related neurons, 2.24 ± 0.11 ms (range, 1.32–2.94 ms) for Type II wake-related neurons and 1.86 ± 0.07 ms (range, 1.44–2.16 ms) for REM-related neurons. There was a significant effect of cell classification on action potential duration ($F_{3,95} = 10.2$, $P < 0.0001$). Mean durations for Type I and Type II wake-related neurons were significantly longer

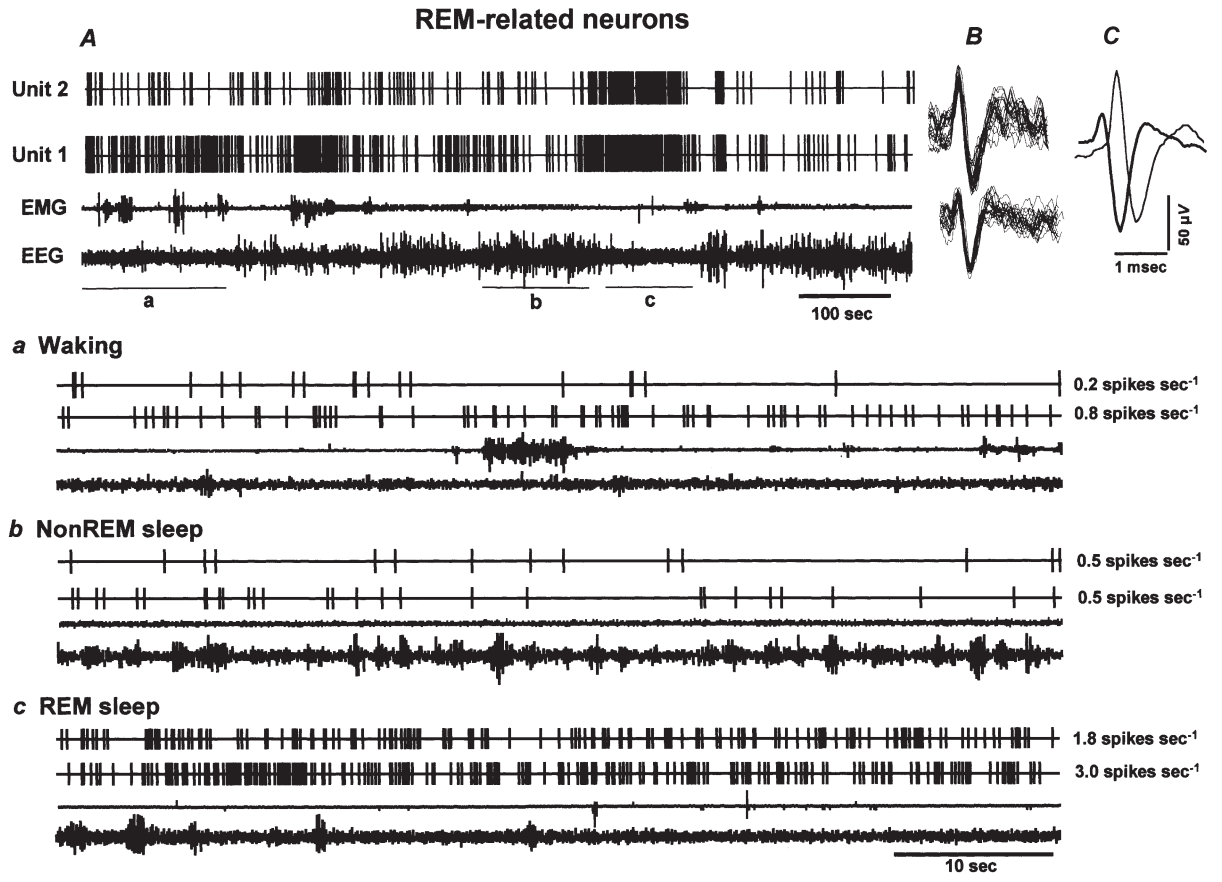

Figure 6. The discharge pattern of individual REM-related neurons across the sleep–waking cycle

A, 15 min continuous recording showing the discharge of two REM-related neurons (Units 1 and 2) recorded simultaneously across the sleep–waking cycle. The superimposed waveforms of individual action potentials captured during 5 s for each recorded neuron along with background noise and their averaged waveforms are shown in *B* and *C*, respectively. Lower panels depict expanded tracings (60 s) from *A*, illustrating the discharge patterns of the two neurons during waking (*a*), non-REM sleep (*b*) and REM sleep (*c*). The values to the right of each expanded tracing represent mean discharge rates of the respective neurons during the representative sections. These neurons exhibited lower discharge rates during waking and non-REM sleep and increased discharge rates during REM sleep.

than for both wake/REM- and REM-related neurons (Newman-Keuls, $P < 0.05$), but did not differ significantly from each other. Mean action potential durations for wake/REM- and REM-related neurons did not differ significantly from each other.

EMG activity *vs.* discharge rate

Relationships between the discharge rate of individual neurons and changes in rectified EMG voltage occurring spontaneously across the sleep–waking cycle for each of the four classes of PF-LHA neuron are shown in Fig. 8. The discharge rate of Type I wake-related neurons showed a strong positive correlation with rectified EMG voltage across all sleep–waking states ($r = 0.48$, $t = 6.43$, $P < 0.001$), as was the case for type II wake-related neurons ($r = 0.18$, $t = 2.95$, $P < 0.01$). The discharge rates of a comparable number of wake/REM-related ($n = 23$) and of REM-related ($n = 10$) neurons were not correlated with EMG voltage ($r = -0.0286$, $t = -0.410$, $P = 0.68$, and $r = -0.019$, $t = -0.597$, $P = 0.551$, respectively).

DISCUSSION

The lateral hypothalamus has been implicated in several waking behaviours, including feeding, drinking and locomotor activity (Teitelbaum & Epstein, 1962; Sinnamon *et al.* 1999). This region has also been implicated in the maintenance of the waking state, i.e. in the behavioural and electrographic manifestations of arousal (de Ryck & Teitelbaum, 1978; Shoham & Teitelbaum, 1982). The unit recording studies carried out in the present study are consistent with a role for the lateral hypothalamus in one or more aspects of waking behaviour, because nearly all PF-LHA neurons that we examined were active during waking, but exhibited significantly reduced activity during non-REM sleep. Furthermore, we found that neurons in the PF-LHA that were active during waking were of two general types, namely those that exhibited similar levels of activation during waking and REM sleep and those that exhibited significantly reduced discharge rates during REM sleep compared to waking.

The discovery that neurons containing the hypocretin (or orexin) peptides are localized in the PF-LHA has generated considerable interest in this region of the hypothalamus (de Lecea *et al.* 1998; Sakurai *et al.* 1998). The available evidence suggests that activation of Hcrt neurons promotes waking, suppresses REM sleep and antagonizes loss of muscle tone during waking. Hcrt neurons exhibit c-fos activation in response to systemic administration of stimulatory drugs and in response to sustained waking (Scammell *et al.* 2000; Estabrooke *et al.* 2001). Central administration of Hcrt in rats acutely increases time spent awake and suppresses non-REM and REM sleep (Bourgin *et al.* 2000). Micro-perfusion of a Hcrt-2 receptor antagonist into the brainstem promotes REM sleep (Thakkar *et al.* 1999). Hcrt exerts excitatory effects on locus coeruleus neurons (Hagan *et al.* 1999; Horvath *et al.* 1999) and these neurons are normally silent during REM sleep (Aston-Jones & Bloom, 1981). Finally, loss of Hcrt-containing neurons in human narcolepsy (Peyron *et al.* 2000; Thannickal *et al.* 2000) and abnormalities in hypocretin receptors in animal models of narcolepsy (Chemelli *et al.* 1999; Lin *et al.* 1999) are associated with excessive sleepiness, reduced latencies to REM sleep onset and the intrusion of the muscle atonia of REM sleep into the waking state (known as cataplexy).

Based on this evidence, we hypothesized that Hcrt neurons should exhibit a wake-related discharge pattern, with peak discharge rates in the waking state and reduced rates during non-REM and REM sleep. Here, we report the presence of neurons with wake-related discharge patterns in regions of the rat PF-LHA that contain Hcrt-immunoreactive neurons. Type I wake-related neurons comprised 23 % of the total number of recorded neurons and Type II wake-related neurons accounted for an additional 15 %.

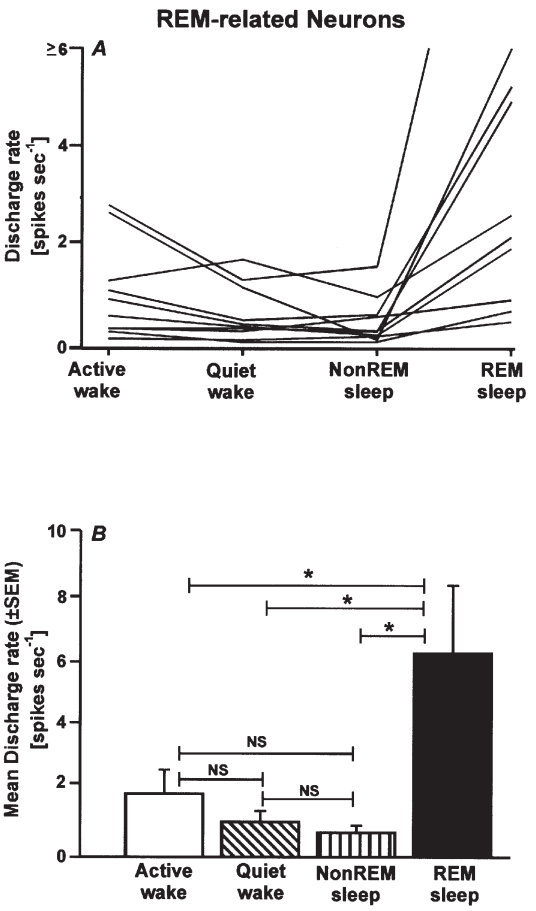

Figure 7. Discharge characteristics of REM-related neurons

Individual (*A*) and mean (± S.E.M.; *B*) discharge rates of REM-related neurons during AW, QW, non-REM sleep and REM sleep. These neurons exhibited low discharge rates during AW, QW and non-REM sleep, with comparatively elevated discharge rates during REM sleep. * $P < 0.01$.

Categorization of wake-related neurons as either Type I or II was based solely on the magnitude of the reduction in discharge rate during REM sleep compared to waking. Type I and II neurons exhibited similar patterns of neuronal discharge across the sleep–waking cycle (Fig. 5) and exhibited nearly identical action potential durations. Therefore, rather than constituting two physiologically distinct types of cell, Type I and II wake-related neurons may reflect two components of the same neuronal population.

For all of the PF-LHA cell types described here, changes in discharge rate during different waking behaviours and across the sleep–waking cycle may reflect changes in excitatory and/or inhibitory synaptic input to these cells, rather than endogenous pacemaker activity.

Based on our reconstructions of the microwire bundle tracks, almost all of the 106 neurons recorded in this study were located within the field of Hcrt-1-immunoreactive neurons. However, the extracellular recording method employed here precludes identification of the neurotransmitter phenotype of recorded neurons. Therefore, we were unable to determine whether Hcrt-producing neurons exhibit the wake/REM-related discharge pattern (Figs 2 and 3), the wake-related discharge pattern (Figs 4 and 5) or the REM-related discharge pattern (Figs 6 and 7).

Kilduff & Peyron (2000) hypothesized that Hcrt-producing neurons exhibit activation during both waking and REM sleep, with diminished activity during non-REM sleep. We recorded several cells in the PF-LHA that exhibited a wake/REM-related discharge pattern. In fact,

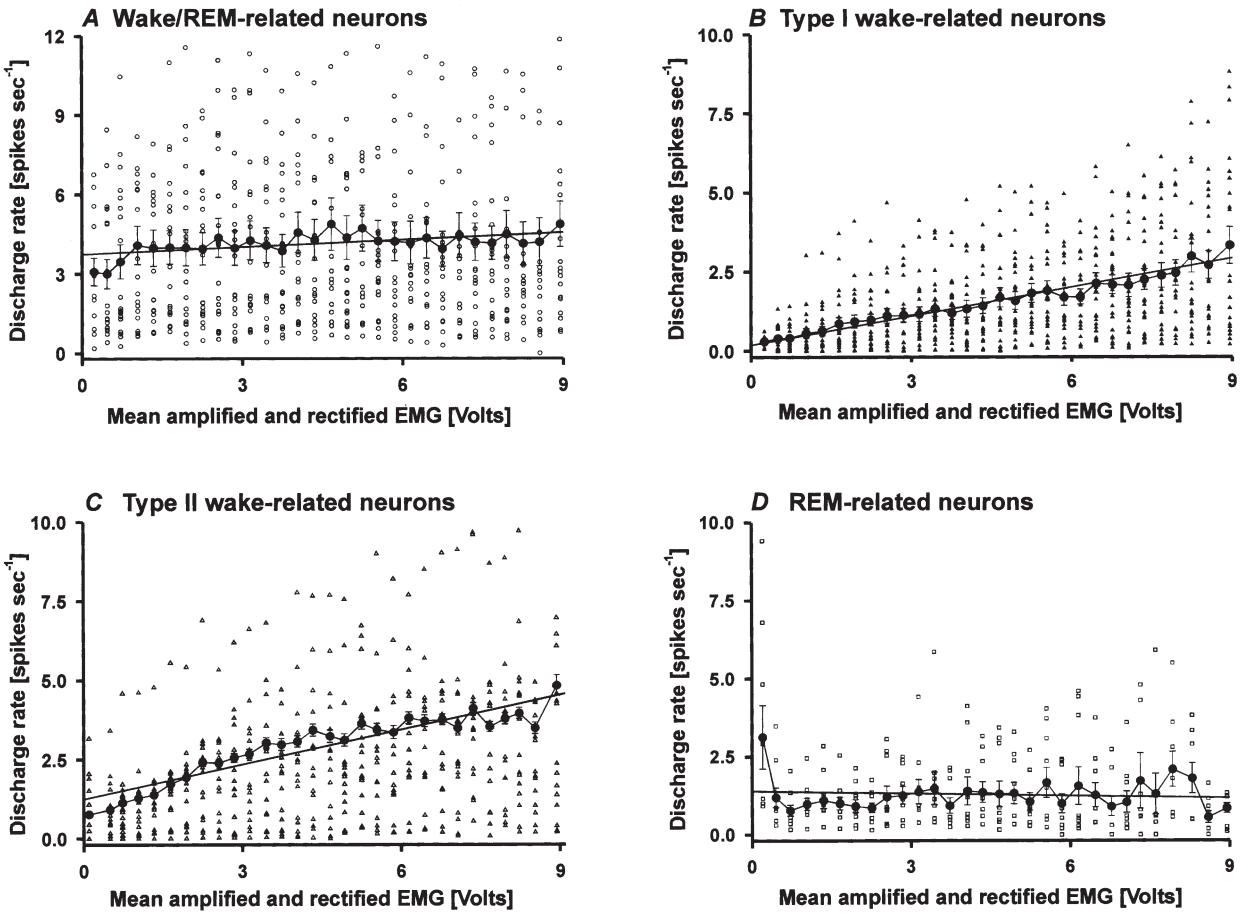

Figure 8. Correlation of PF-LHA neuronal activity with muscle activity

Correlation between discharge rate and EMG activity of wake/REM-related (*A*), Type I wake-related (*B*), Type II wake-related (*C*) and REM-related (*D*) neurons. Mean (± S.E.M.) discharge rates of individual neurons (large filled circles) are plotted against mean rectified and amplified EMG voltages calculated during successive 5 s epochs across 3–5 sleep–waking cycles. Discharge rates were divided into 0.3 V bins. The straight line in each graph represents the simple linear regression between discharge rate and EMG voltage. The discharge rates of Type I and II wake-related neurons (*B* and *C*) were strongly positively correlated with EMG voltage across all sleep–waking states. The discharge rates of a comparable number of wake/REM-related neurons ($n = 23$) and of REM-related neurons were not significantly correlated with EMG voltage.

these were the most commonly encountered neurons, as is the case in more posterior regions of the lateral hypothalamus (Szymusiak *et al.* 1989; Krilowicz *et al.* 1994; Steininger *et al.* 1999). As a group, wake/REM-related cells exhibited a significant reduction in discharge rate during non-REM sleep compared to AW, QW and REM sleep and, therefore, fit the state-dependent discharge profile predicted by Kilduff & Peyron (2000) for Hcrt cells.

Regardless of which of the state-dependent discharge patterns defined here on the basis of the REM/wake discharge rate ratio is eventually found to be typical of Hcrt-producing neurons, it seems probable that Hcrt-producing neurons comprise only a subset of the neurons recorded in the present study. Hcrt-producing neurons in the PF-LHA are interspersed with other cell types, including neurons that contain MCH (Broberger *et al.* 1998; Peyron *et al.* 1998). Hcrt-producing neurons are outnumbered by non-Hcrt cells throughout the PF-LHA (Peyron *et al.* 1998). Therefore, assuming a random sampling of cell types in the present study, only a minority of cells that were recorded from microelectrode passes through this region would be Hcrt neurons. Given the relatively high percentage of wake-related neurons that we encountered in the PF-LHA (38 %), it seems plausible that this discharge pattern is not confined to PF-LHA cells with a single neurotransmitter phenotype.

Neurons with wake-related discharge patterns (also referred to as 'REM-off' neurons) have been most extensively characterized in brain regions that contain monoaminergic neurons. These include the serotonergic neurons in the dorsal raphe nuclei (McGinty & Harper, 1976; Jacobs & Fornal, 1999; Guzman-Marin *et al.* 2000), noradrenergic neurons of the locus coeruleus (Aston-Jones & Bloom, 1981) and histaminergic neurons in the tuberomammillary nuclei of the posterior hypothalamus (Vanni-Mercier *et al.* 1984; Steininger *et al.* 1999). Wake-related neurons recorded in the PF-LHA in the present study exhibit both similarities to and differences from the discharge patterns described for monoaminergic neurons. For example, the magnitude of suppression of discharge during REM sleep compared to AW was similar for PF-LHA Type I wake-related neurons and putative serotonergic neurons in the dorsal raphe nucleus (Table 1). However, the discharge of PF-LHA neurons was more strongly modulated from AW to QW than has been described for monoaminergic neurons in the dorsal raphe and other regions. Another characteristic of putative serotonergic neurons is a progressive decline in discharge rate from light to deep non-REM sleep and a further significant decrease in discharge rate from deep non-REM to REM sleep (Lydic *et al.* 1985; Guzman-Marin *et al.* 2000). However, PF-LHA wake-related neurons did not show a significant reduction in discharge rate from QW to non-REM sleep to REM sleep in the present study. Therefore, it appears that wake/REM-related neurons in the PF-LHA are more selectively active during AW than wake-related neurons recorded in monoaminergic brain regions.

The increased discharge rates of PF-LHA wake-related neurons during AW compared to QW prompted us to examine the relationship between neuronal discharge and muscle activity across each of the sleep and waking states. The discharge rates of both Type I and Type II wake-related neurons exhibited strong positive correlations with muscle activity (Fig. 8), whereas the discharge rates of the other two classes of neuron did not. The correlation between PF-LHA wake-related neuronal activity and muscle activity suggests a role for these cells in motor control, behavioural arousal and/or the regulation of muscle activity across the sleep–waking cycle.

REFERENCES

Alam, M. N., McGinty, D. & Szymusiak, R. (1997). Thermosensitive neurons of the diagonal band in rats: relation to wakefulness and non-rapid eye movement sleep. *Brain Research* **752**, 81–89.

Aston-Jones, G. & Bloom, F. E. (1981). Activity of norepinepherine-containing locus coeruleus neurons in behaving rats anticipates fluctuations in the sleep–waking cycle. *Journal of Neuroscience* **1**, 876–886.

Bittencourt, J. C., Frigo, L., Rissman, R. A., Casatti, C. A., Nahon, J. L. & Bauer, J. A. (1998). The distribution of melanin-concentrating hormone in the monkey brain (*Cebus apella*). *Brain Research* **804**, 140–143.

Bittencourt, J. C., Presse, F., Arias, C., Peto, C., Vaughan, J., Nahon, J. L., Vale, W. & Sawchenko, P. E. (1992). The melanin-concentrating hormone system of the rat brain: an immuno- and hybridization histochemical characterization. *Journal of Comparative Neurology* **319**, 218–245.

Bourgin, P., Huitron-Resendiz, S., Spier, A. D., Fabre, V., Morte, B., Criado, J. R., Sutcliffe, J. G., Henriksen, S. J. & De Lecea, L. (2000). Hypocretin-1 modulates rapid eye movement sleep through activation of locus coeruleus neurons. *Journal of Neuroscience* **20**, 7760–7765.

Broberger, C., De Lecea, L., Sutcliffe, J. G. & Hokfelt, T. (1998). Hypocretin/orexin- and melanin-concentrating hormone-expressing cells form distinct populations in the rodent lateral hypothalamus: relationship to the neuropeptide Y and agouti gene-related protein systems. *Journal of Comparative Neurology* **402**, 460–474.

Chemelli, R. M., Willie, J. T., Sinton, C. M., Elmquist, J. K., Scammell, T., Lee, C., Richardson, J. A., Williams, S. C., Xiong, Y., Kisanuki, Y., Fitch, T. E., Nakazato, M., Hammer, R. E., Saper, C. B. & Yanagisawa, M. (1999). Narcolepsy in orexin knockout mice: molecular genetics of sleep regulation. *Cell* **98**, 437–451.

de Lecea, L., Kilduff, T. S., Peyron, C., Gao, X., Foye, P. E., Danielson, P. E., Fukuhara, C., Battenberg, E. L., Gautvik, V. T., Bartlett, F. S., Frankel, W. N., van den Pol, A. N., Bloom, F. E., Gautvik, K. M. & Sutcliffe, J. G. (1998). The hypocretins: hypothalamus-specific peptides with neuroexcitatory activity. *Proceedings of the National Academy of Sciences of the USA* **95**, 322–327.

De Ryck, M. & Teitelbaum, P. (1978). Neocortical and hippocampal EEG in normal and lateral hypothalamic damaged rats. *Physiology and Behavior* **20**, 403–409.

Estabrooke, I. V., McCarthy, M. T., Ko, E., Chou, T. C., Chemelli, R. M., Yanagisawa, M., Saper, C.B. & Scammell, T. E. (2001). Fos expression in orexin neurons varies with behavioral state. *Journal of Neuroscience* **21**, 1656–1662.

Guzman-Marin, R., Alam, M. N., Szymusiak, R., Drucker-Colin, R. & McGinty, D. (2000). Discharge modulation of rat dorsal raphe neurons during sleep and waking: effects of preoptic/basal forebrain warming. *Brain Research* **875**, 23–34.

Hagan, J. J., Leslie, R. A., Patel, S., Evans, M. L., Wattam, T. A., Holmes, S., Benham, C .D., Taylor, S. G., Routledge, C., Hemmati, P., Munton, R. P., Ashmeade, T. E., Shah, A. S., Hatcher, J. P., Hatcher, P. D., Jones, D. N., Smith, M. I., Piper, D. C., Hunter, A. J., Porter, R. A. & Upton, N. (1999). Orexin A activates locus coeruleus cell firing and increases arousal in the rat. *Proceedings of the National Academy of Sciences of the USA* **96**, 10911–10916.

Horvath, T. L., Peyron, C., Diano, S., Ivanov, A., Aston-Jones, G., Kilduff, T. S. & van den Pol, A. N. (1999). Hypocretin (orexin) activation and synaptic innervation of the locus coeruleus noradrenergic system. *Journal of Comparative Neurology* **415**, 145–159.

Jacobs, B. L. & Fornal, C. A. (1999). Activity of serotonergic neurons in behaving animals. *Neuropsychopharmacologyy* **21**, 9–15S.

Kilduff, T. S. & Peyron, C. (2000). The hypocretin/orexin ligand-receptor system: implications for sleep and sleep disorders. *Trends in Neurosciences* **23**, 359–365.

Krilowicz, B. L., Szymusiak, R. & McGinty, D. (1994). Regulation of posterior lateral hypothalamic arousal related neuronal discharge by preoptic anterior hypothalamic warming. *Brain Research* **668**, 30–38.

Krolicki, L., Chodobski, A. & Skolasinska, K. (1985). The effect of stimulation of the reticulo-hypothalamic-hippocampal systems on the cerebral blood flow and neocortical and hippocampal electrical activity in cats. *Experimental Brain Research* **60**, 551–558.

Leibowitz, S. F. (1986). Brain monoamines and peptides: role in the control of eating behavior. *Federation Proceedings* **45**, 1396–1403.

Levitt, D. R. & Teitelbaum, P. (1975). Somnolence, akinesia and sensory activation of motivated behavior in the lateral hypothalamic syndrome. *Proceedings of the National Academy of Sciences of the USA* **72**, 2819–2823.

Lin, L., Faraco, J., Li, R., Kadotani, H., Rogers, W., Lin, X., Qiu, X., De Jong, P.J., Nishino, S. & Mignot, E. (1999). The sleep disorder canine narcolepsy is caused by a mutation in the hypocretin (orexin) receptor 2 gene. *Cell* **98**, 365–376.

Lydic, R., McCarley, R. W. & Hobson, J. A. (1985). The time course of dorsal raphe discharge, PGO waves, and muscle tone averaged across multiple sleep–wake cycles. *Experimental Brain Research* **12**, 131–144.

McGinty, D. & Harper, R. M. (1976). Dorsal raphe neurons: depression of firing during sleep in cats. *Brain Research* **101**, 569–575.

Marshall, J. F. & Teitelbaum, P. (1974). Further analysis of sensory inattention following lateral hypothalamic damage in rats. *Journal of Comparative and Physiological Psychology* **86**, 375–395.

Methippara, M. M., Alam, M. N., Szymusiak, R. & McGinty, D. (2000). Effects of lateral preoptic area application of orexin-A on sleep-wakefulness. *NeuroReport* **11**, 3423–3426.

Nambu, T., Sakurai, T., Mizukami, K., Hosoya, Y., Yanagisawa, M. & Goto, K. (1999). Distribution of orexin neurons in the adult rat brain. *Brain Research* **827**, 243–260.

Paxinos, G. & Watson, C. (1998). *The Rat Brain in Stereotaxic Coordinates*. Academic Press, San Diego.

Peyron, C., Faraco, J., Rogers, W., Ripley, B., Overeem, S., Charnay, Y., Nevsimalova, S., Aldrich, M., Reynolds, D., Albin, R., Li, R., Hungs, M., Pedrazzoli, M., Padigaru, M., Kucherlapati, M., Fan, J., Maki, R., Lammers, G. J., Bouras, C., Kucherlapati, R., Nishino, S. & Mignot, E. (2000). A mutation in a case of early onset narcolepsy and a generalized absence of hypocretin peptides in human narcoleptic brains. *Nature Medicine* **6**, 991–997.

Peyron, C., Tighe, D. K., van den Pol, A. N., de Lecea, L., Heller, H. C., Sutcliffe, J. G. & Kilduff, T. S. (1998). Neurons containing hypocretin (orexin) project to multiple neuronal systems. *Journal of Neuroscience* **18**, 9996–10015.

Piper, D. C., Upton, N., Smith, M. I. & Hunter, A. J. (2000). The novel brain neuropeptide, orexin-A, modulates the sleep–wake cycle of rats. *European Journal of Neuroscience* **12**, 726–730.

Qu, D., Ludwig, D. S., Gammeltoft, S., Piper, M., Pelleymounter, M. A., Cullen, M. J., Mathes, W. F., Przypek, R., Kanarek, R. & Maratos-Flier, E. (1996). A role for melanin-concentrating hormone in the central regulation of feeding behaviour. *Nature* **380**, 243–247.

Sakurai, T., Amemiya, A., Ishii, M., Matsuzaki, I., Chemelli, R. M., Tanaka, H., Williams, S. C., Richardson, J. A., Kozlowski, G. P., Wilson, S., Arch, J. R., Buckingham, R. E., Haynes, A. C., Carr, S. A., Annan, R. S., McNulty, D. E., Liu, W. S., Terrett, J. A., Elshourbagy, N. A., Bergsma, D. J. & Yanagisawa, M. (1998). Orexins and orexin receptors: a family of hypothalamic neuropeptides and G protein-coupled receptors that regulate feeding behavior. *Cell* **92**, 573–585.

Scammell, T. E., Estabrooke, I. V., McCarthy, M. T., Chemelli, R. M., Yanagisawa, M., Miller, M. S. & Saper, C. B. (2000). Hypothalamic arousal regions are activated during modafinil-induced wakefulness. *Journal of Neuroscience* **20**, 8620–8628.

Shoham, S. & Teitelbaum, P. (1982). Subcortical waking and sleep during lateral hypothalamic 'somnolence' in rats. *Physiology and Behavior* **28**, 323–334.

Siegel, J. M. (2000). Narcolepsy. *Scientific American* **282**, 58–63.

Sinnamon, H. M., Karvosky, M. E. & Ilch, C. P. (1999). Locomotion and head scanning initiated by hypothalamic stimulation are inversely related. *Behavioral Brain Research* **99**, 219–229.

Stanley, B. G., Chin, A. S. & Leibowitz, S. F. (1985). Feeding and drinking elicited by central injection of neuropeptide Y: evidence for a hypothalamic site(s) of action. *Brain Research Bulletin* **14**, 521–524.

Steininger, T. L., Alam, M. N., Gong, H., Szymusiak, R. & McGinty, D. (1999). Sleep-waking discharge of neurons in the posterior lateral hypothalamus of the albino rat. *Brain Research* **840**, 138–147.

Stock, G., Rupprecht, U., Stumpf, H. & Schlor, K. H. (1981). Cardiovascular changes during arousal elicited by stimulation of amygdala, hypothalamus and locus coeruleus. *Journal of the Autonomic Nervous System* **3**, 503–510.

Szymusiak, R., Iriye, T. & McGinty, D. (1989). Sleep-waking discharge of neurons in the posterior lateral hypothalamic area of cats. *Brain Research Bulletin* **23**, 111–120.

Teitelbaum, P. & Epstein, A. (1962). Recovery of feeding and drinking after lateral hypothalamic lesions. *Psychological Reviews* **69**, 74–90.

Thakkar, M. M., Ramesh, V., Cape, E. G., Winston, S., Strecker, R. E. & McCarley, R. W. (1999). REM sleep enhancement and behavioral cataplexy following orexin (hypocretin)-II receptor antisense perfusion in the pontine reticular formation. *Sleep Research Online* **2**, 113–120.

Thannickal, T. C., Moore, R. Y., Nienhuis, R., Ramanathan, L., Gulyani, S., Aldrich, M., Cornford, M. & Siegel, J. M. (2000). Reduced number of hypocretin neurons in human narcolepsy. *Neuron* **27**, 469–474.

Timo-Iaria, C., Negrao, N., Schmidek, W. R., Hoshino, K., Demenezes, C. E. L. & Darocha, T. L. (1970). Phases and states of sleep in rat. *Physiology and Behavior* **5**, 1057–1062.

Vanni-Mercier, G., Sakai, K. & Jouvet, M. (1984). Neurons specifiques de l'eveil dans l'hypothalamus posterior du chat. *Comptes rendus Academie des Sciences* **298**, 195–200.

Yamamoto, Y., Ueta, Y., Serino, R., Nomura, M., Shibuya, I. & Yamashita, H. (2000). Effects of food restriction on the hypothalamic prepro-orexin gene expression in genetically obese mice. *Brain Research Bulletin* **51**, 515–521.

Acknowledgements

This research was supported by the US Department of Veterans Affairs Medical Research Service and US National Institutes of Health grants MH 47480, MH 61354 and HL 60296.